Hindawi Publishing Corporation
Journal of Nanomaterials
Volume 2010, Article ID 740628, 6 pages
doi:10.1155/2010/740628

Research Article

Controlled Synthesis of ZnO Nanostructures by Electrodeposition Method

Gong Jiangfeng,[1,2] Dou Zhaoming,[1] Ding Qingping,[3] Xu Yuan,[1] and Zhu Weihua[1]

[1] *Department of Physics, Hohai University, Nanjing 210098, China*
[2] *National Laboratory of Solid State Microstructures, Nanjing University, Nanjing 210093, China*
[3] *School of Physical Electronics, University of Electronic Science and Technology of China, Chengdu 610054, China*

Correspondence should be addressed to Gong Jiangfeng, jfgong@hhu.edu.cn

Received 25 August 2010; Accepted 18 October 2010

Academic Editor: Xuedong Bai

We present here a systematic study on the synthesis of various ZnO nanostructures by electrodeposition method with $ZnCl_2$ solution as starting reactant. Several reaction parameters were examined to develop an optimal procedure for controlling the size, shape, and surface morphology of the nanostructure. The results showed that the morphology of the products can be carefully controlled through adjusting the concentration of the electrolyte. The products present well-aligned nanorod arrays when the concentration is low. However, they act as anomalous hexangular nanoplates when the concentration of $ZnCl_2$ is higher than 5 mM. Transmission electron microscopy and select area electron diffraction results show that the product presents good crystallinity. A possible formation process has been proposed.

1. Introduction

ZnO is a well-known II–VI semiconductor; it has a direct band gap in the ultraviolet range (3.37 eV) and a large exciton binding energy (60 meV), which made it a great application prospect due to its extrusive physical properties. With the help of the discovery of carbon nanotubes, nanostructures and nanomaterials have attracted great interest in the recent years. Zinc oxide nanostructures have become attractive building blocks for devices in light-emitting diodes, solar cells, sensors, field emitters, and piezoelectric devices in recent years [1–6]. The reports of ZnO nanobelts [7] and nanolasers [8] have spurred a great interest in studies on the synthesis and applications of ZnO nanostructures. It has been shown that band edge, exciton energies, and UV luminescence of ZnO nanostructures are affected by crystallite size and crystal morphology [9–11]. In order to exploit this broad range of applications, it is desirable to tailor the electronic properties of ZnO.

Various techniques have been used to prepare ZnO nanostructures, such as arc discharge, laser vaporization, pyrolysis, physical vapor deposition, chemical vapor deposition (CVD), and soft chemical method [12–21]. Generally, ZnO nanostructures are prepared by high-temperature solidification methods from the vapor-phase elements in vacuum condition. Usually, catalysts such as Au and Co have also been introduced into the synthesis process to orient ZnO nanowires growth. The above-mentioned synthesis method has some disadvantages. (1) Usually, the synthesis process is going under high temperature, which may limit its applied field. (2) The physical properties of ZnO nanostructures can be affected due to the catalysts used in experiment. Therefore, it is still a challenge to synthesize ZnO nanostructures under lower temperature.

Electrodeposition technique is now emerging as an important method to prepare semiconductor thin films. Preparation of oxide films by electrodeposition from aqueous solution presents several advantages over other techniques; this method presents interesting characteristics for large-area, low-cost, and generally low-temperature and soft processing of materials. It has been reported that a wurtzite ZnO film with high optical transparency can be prepared by

cathodal deposition from a simple zinc nitrate [$Zn(NO_3)_2$] aqueous solution [22–25].

In the present work, the potentiostatic method was chosen to obtain the ZnO nanorod films on several kinds of substrates. The influence of growth conditions such as deposition potential and concentration of constituents of the bath on the morphology of reaction products and composition was investigated.

2. Experimental Details

All chemicals were from commercial sources, and they were used without further purification. All solutions in this study were prepared from deionized water.

The working substrates used in the experiment are gold-coated silicon, indium-doped tin oxide (ITO), and copper strip. They were cleaned ultrasonically in detergent, deionized water, and ethanol prior to the film deposition. The Si substrates are high resistant with (111) orientation, which were cut into strips with width and length 1.0 cm and 2.0 cm, respectively. The ITO substrate had a sheet resistance of 10 Ω/square, which was cut into strips with width and length 1.0 cm and 2.0 cm, respectively. The copper slices (0.70 cm × 2 cm) were polished on 1 μm sand paper for 10 min and then cleaned as described above.

In a typical procedure, the electrodeposition was carried out in a three-electrode cell system, in which the working substrates were used as the working electrode, saturated calomel electrode (SCE) serving as reference electrode, and the Zinc slice working as the count electrode, which was used to maintain a constant Zn ion concentration during the electrodeposition. The ZnO nanorod films were cathodically electrodeposited from baths containing different molar ratios of $ZnCl_2$ in 0.1 M KCl dissolved in the deionized water as supporting electrolyte. The bath temperature was maintained at 70°C by using a thermostat. The ZnO films were electrodeposited under potentiostatic condition of −1.0 V (versus SCE) for 90 minutes.

The crystallographic characterization of as-prepared samples was carried out by an X-ray diffractometer (XRD, D/max 2550 v, Cu K radiation). Morphology of the films was observed using a field emission scanning electron microscope (F-SEM, LEO1530VP, Germany), operated at an acceleration voltage of 20 kV. Transmission electron microscopic (TEM) images were performed with a high-resolution transmission electron microscope (HRTEM, Tacnail-F20 operated at 200 kV, FEI, USA). The HRTEM was equipped with a Gatan multiscan charge-coupled device (CCD) camera system (Model 794, Gatan Inc., Pleasanton, CA, USA) to record the HRTEM images and SAED patterns. Chemical composition of the as-prepared samples was obtained using an energy-dispersive spectrometer (EDS, DEAX, USA).

3. Results and Discussion

In the process of electrodeposition, there are mainly two parts: solution chemistry process and electrochemistry process, respectively. First, precursor dissolved in the water formed electrolyte, which contains mass of zinc cation and other anion. Secondly, the basic reaction of oxygen reduction on the surface of substrates leads to hydroxide ions formation, then the zinc hydroxide, generated by OH^- absorbed on or near the substrates surfaces and Zn^{2+} in the electrolytes, could be transformed into zinc oxide when the solution temperature is higher than 39°C under low pressure-conditions (720 Pa) [18]. The possible reactions for the ZnO nanorod film formation are

$$\begin{aligned} O_2 + 2H_2O + 4e^- &= 4OH^-, \\ Zn^{2+} + 2OH^- &= Zn(OH)_2, \\ Zn(OH)_2 &= ZnO + H_2O. \end{aligned} \tag{1}$$

The electrochemical reaction is mainly determined by the electrodeposition potential. Figure 1 gives the F-SEM

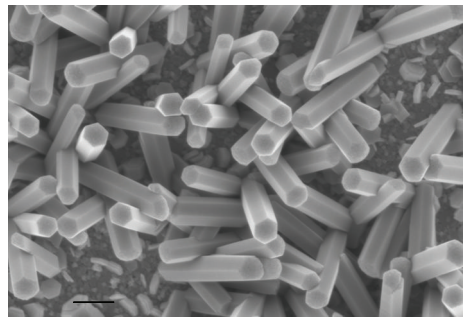

(a)

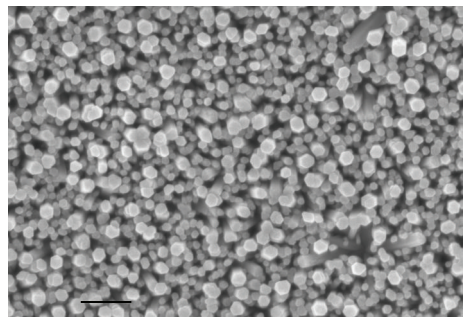

(b)

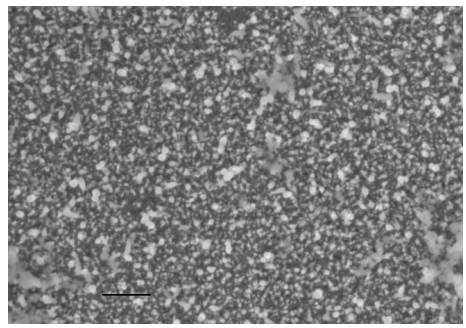

(c)

Figure 1: F-SEM images of ZnO nanorod film electrodeposited under different potentials: (a) $E = -0.7$ V, (b) $E = -1.0$ V, (c) and $E = -1.3$ V. Preparing conditions: $T = 70°C$, $t = 90$ min, and Zn 2+ = 1 mM. The scale bar is 300 nm.

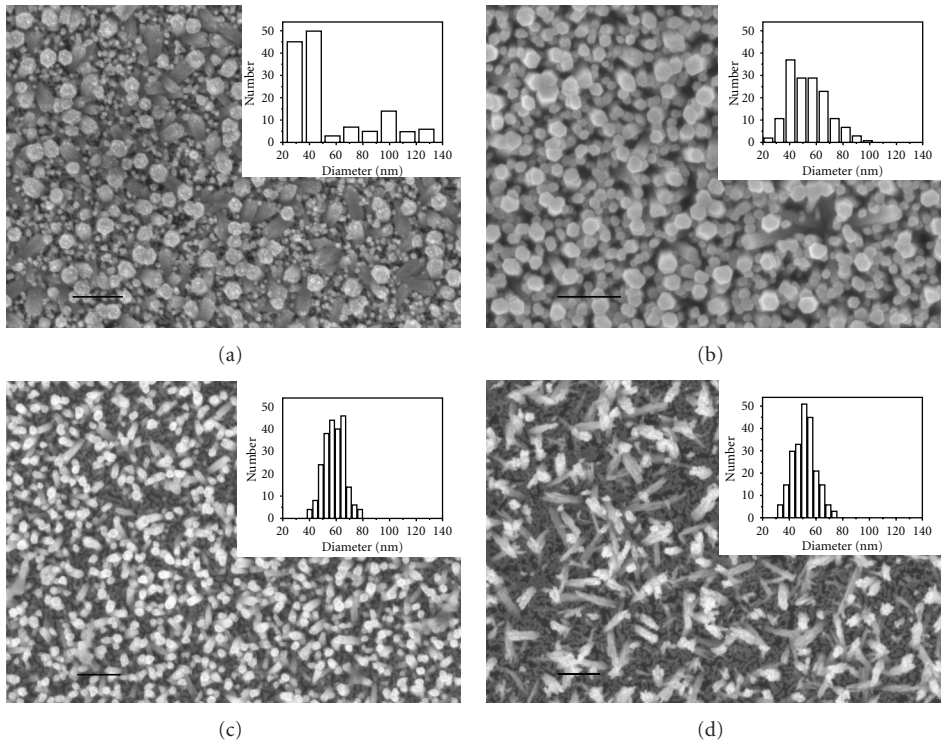

Figure 2: F-SEM image of a ZnO film electrodeposited under different ZnCl2 concentrations: (a) 5 mM, (b) 1 mM, (c) 0.5 mM, and (d) 0.2 mM. Other preparing conditions are $E = -1.0$ V, $T = 70^{\circ}$C, and $t = 90$ min. The scale bar is 300 nm.

images of ZnO nanorod films electrodeposited under the following different potentials, for example, −0.7, −1.0 and −1.3 V. It can be seen from Figure 1(a) that ZnO nanorods were formed on the electrode when the applied potential was controlled at −0.7 V, and the synthesized ZnO nanorods had uniform diameter and length. However, not all the nanorods were perpendicular to the substrate and some gap appeared. When the electrodeposition potential reduced to −1.0 V, the product as shown in Figure 1(b), the diameter of the nanorods decreased form 140 nm to 60 nm rapidly, and dense ZnO nanorods film were formed. When the reduction potential was reduced to −1.3 V, only agglomerated ZnO nanoparticles were irregularly distributed on the substrates, indicating that few hydroxide ions were generated on the surface of substrates. Therefore, the growth rate of ZnO nanorods is relatively lower at this potential.

In order to study the influence of the electrolyte, the films were deposited with various zinc ions concentrations, while retaining a constant applied potential of −1.0 V and a temperature 70°C. The deposition time of the samples was ∼90 min. After the deposition experiments, the deposits were washed with distilled water several times. Visually, a dark grey, well-adherent deposit was obtained after potentiostatic deposition. Figure 2 shows the top view F-SEM micrographs of representative ZnO nanorods films deposited on Au-coated silicon substrates. The zinc ions concentrations used in the experiment are 5 mM, 1 mM, 0.5 mM, and 0.2 mM; the results are displayed in Figures 2(a)–2(d), respectively. As we can see, the diameters and densities of the nanorods are strongly dependent on the zinc ions concentration. When the zinc ions concentration is higher (5 mM) and the deposits present as dense nanorod films, careful analysis found that the diameter of the nanorods was in bimodal distribution, with one peak value at 35 nm and the other peak value at 90 nm. While the concentration of zinc ions decreased from 5 mM to 1 mM, the ZnO with relatively higher density was formed, the diameter of the nanorods distributed in a broad range from 20 nm to 100 nm, which present unimodal distribution, and the average diameter decreased to about 60 nm. When the concentration of zinc ion decreased to 0.5 mM, the average diameter kept at 58 nm while the diameters distributed in relatively narrow range. When the concentration is reduced to an even lower degree, the ZnO nanorods lay on the substrate desultorily and the average diameter is 53 nm. This fact indicated that the compound formation mainly depends on the zinc ions concentration and the well-aligned ZnO nanorods with uniform diameter can be fabricated when the concentration of zinc ions is 1 mM. The low supersaturation degree is believed to be responsible for the small diameter and the narrow size distribution of the ZnO nanorod electrodeposited in solution with relatively low concentration. The detailed statistical results of the influence of zinc concentration on average diameter are shown as insert in Figure 2.

X-ray diffraction pattern of ZnO nanorod films deposited at Au-coated Si substrate is shown in Figure 3. The zinc chloride concentration and deposition potential were maintained at 1 mM and −1.0 V, respectively. The

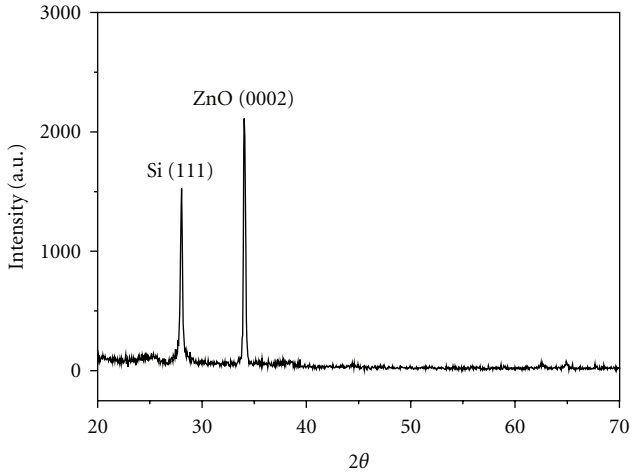

Figure 3: XRD pattern of the ZnO film electrodeposited with ZnCl2 concentration 1 mM and electrochemical potential $E = -1.0$ V.

appearance of several peaks in the XRD reveals that the films are polycrystalline in nature and the structure is identified to be hexagonal phase (JCPDS no. 361451). The most intense peak with small line width corresponds to (0002) plane in the XRD which indicates a good crystallization state. The strong preferential orientation along the (0002) direction (c-axis) perpendicular to the substrate is consistent with the growth habit generally evidenced for ZnO films deposited by other deposition methods from the gas phase. As seen from the XRD, some peak attributed to the Si substrate could be clearly observed, which indicates that the thickness is lower and the films are not compact enough prepared under this condition. Lattice constant calculated from peak angles is 5.22 Å in the c-axis.

Figure 4 is the TEM images of the typical nanorods and the corresponding SAED pattern. The TEM images were taken by scraping the rods from the substrate and dispersing them in acetone. The images are for rods grown at the following conditions: $ZnCl_2$ concentration is 1 mM, $E = -1.0$ V, $T = 70^{\circ}$C, and $t = 90$ min. The SAED pattern indicated that ZnO nanorods have a hexagonal Wurtzite structure. Figure 4(b) is a high-resolution TEM image taken from the tip of the nanorod, which shows perfect lattice structure. The lattice spacings are 0.520 nm and 0.281 nm, corresponding to the separation between two (0001) lattice planes and two (2-1-10) lattice planes of hexagonal ZnO, respectively. The results indicated that the growth direction of ZnO nanorod is [0001] direction. The EDX result shows that the product is composed of O and Zn with atomic ratio close to 1 : 1, and C and Cu signals come from supporting film.

As a wide-band gap semiconductor, ZnO is regarded as a good candidate in the field of photoluminescence (PL). Figure 5 shows the PL result of the ZnO nanorod arrays. A strong UV emission peak at about 380 nm and a weak green emission band were observed. The UV peak was the characteristic emission of ZnO and was attributed to the excitonic recombination of the near-bandedge emission [26, 27]. The presence of pronounced room temperature

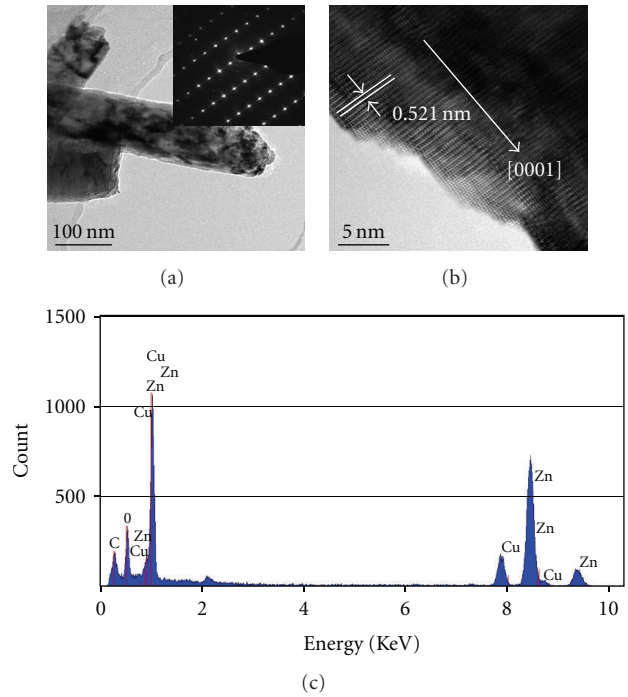

Figure 4: TEM image of the electrodeposited ZnO film. (a) Typical TEM image of single ZnO nanorod; the insert is ED pattern. (b) High-resolution TEM image of ZnO. (c) Corresponding EDS image of ZnO nanorod.

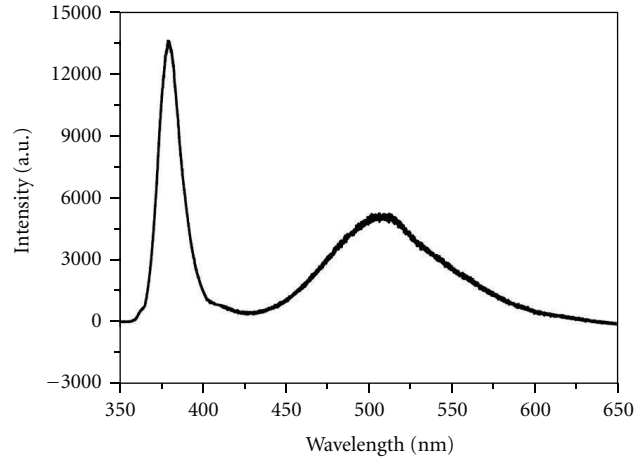

Figure 5: PL spectra of ZnO nanorod film with ZnCl2 concentration 1 mM and electrochemical potential $E = -1.0$ V.

emission in ZnO nanorod arrays indicates that they have a very high structural perfection. The weak green emission is usually attributed to deep energy level defects related to singly ionized oxygen vacancy, which originated from the recombination of a photogenerated hole with a singly ionized charge state of the specific defect [28, 29].

4. Conclusion

In this paper, well-aligned ZnO nanorod films were synthesized successfully via electrodeposition method; we studied

the effects of electrodeposition parameters on the preparation of ZnO nanorod films systematically. Our results indicated that the diameter and the density of the ZnO nanorods depended on the applied potential and Zn2+ concentration, the average diameter of the nanorods decreased as the electrodeposition potential became more negative, and the optimized potential was −1.0 V; when the concentration of precursors decreased, the average diameter of ZnO decreased, which means that the well-aligned ZnO nanorod with uniform diameter can be fabricated at relatively low concentration and the optimized concentration is about 1 mM. TEM studies show that the ZnO nanorods were well crystallized with preferential orientation along the [0002] direction, which is perpendicular to the substrate surface. This kind of ZnO film can be of interest for both fundamental studies and industrial applications.

Acknowledgments

This work was supported by National Natural Science Foundation of China (Grant no. 11004047), China Postdoctoral Sustentation Fund (Grant no. 200904501062), Jiangsu Province Postdoctoral Sustentation Fund, China (Grant no. 0901001B); Talented Faculty Fund of Hehai University (Grant no. 2084/40801131), and the Fundamental Research Funds for Central Universities (B1030095).

References

[1] S. T. Tan, X. W. Sun, J. L. Zhao et al., "Ultraviolet and visible electroluminescence from n-ZnOSi Ox (n,p)—Si heterostructured light-emitting diodes," *Applied Physics Letters*, vol. 93, no. 1, Article ID 013506, 3 pages, 2008.

[2] Y. F. Hsu, Y. Y. Xi, A. B. Djurišić, and W. K. Chan, "ZnO nanorods for solar cells: hydrothermal growth versus vapor deposition," *Applied Physics Letters*, vol. 92, no. 13, Article ID 133507, 3 pages, 2008.

[3] J. H. He, C. H. Ho, and C. Y. Chen, "Polymer functionalized ZnO nanobelts as oxygen sensors with a significant response enhancement," *Nanotechnology*, vol. 20, no. 6, Article ID 065503, 2009.

[4] Z. Hui, D. Ning, C. Bingdi, L. Dongshen, and Y. Deren, "Carbon nanotube-ZnO nanosphere heterostructures: low-temperature chemical reaction synthesis, photoluminescence, and their application for room temperature NH3 gas sensor," *Science of Advanced Materials*, vol. 1, no. 1, pp. 13–17, 2009.

[5] H. Yu, S. Wang, N. Li et al., "MOVPE growth of AlGaN/GaN superlattices on ZnO substrates for green emitter applications," *Journal of Crystal Growth*, vol. 310, no. 23, pp. 4904–4907, 2008.

[6] H. J. Fan, W. Lee, R. Hauschild et al., "Template-assisted large-scale ordered arrays of ZnO pillars for optical and piezoelectric applications," *Small*, vol. 2, no. 4, pp. 561–568, 2006.

[7] Z. W. Pan, Z. U. R. Dai, and Z. L. Wang, "Nanobelts of semiconducting oxides," *Science*, vol. 291, no. 5510, pp. 1947–1949, 2001.

[8] M. H. Huang, S. Mao, H. Feick et al., "Room-temperature ultraviolet nanowire nanolasers," *Science*, vol. 292, no. 5523, pp. 1897–1899, 2001.

[9] T.-L. Phan, S. C. Yu, R. Vincent, N. H. Dan, and W. S. Shi, "Photoluminescence properties of various CVD-grown ZnO nanostructures," *Journal of Luminescence*, vol. 130, no. 7, pp. 1142–1146, 2010.

[10] L. Irimpan, V.P.N. Nampoori, and P. Radhakrishnan, "Optical limiting in ZnO nanocomposites," *Science of Advanced Materials*, vol. 2, no. 4, pp. 578–582, 2010.

[11] K. Zhu, Z. Yan, and W. Chen, "Fabrication of hourglass-like ZnO particles with enhanced blue emission," *Journal of Nanoscience and Nanotechnology*, vol. 10, no. 10, pp. 6594–6598, 2010.

[12] X.-F. Wu, C.-X. Xu, G.-P. Zhu, and Y.-M. Ling, "ZnO nanorods produced by the method of arc discharge," *Chinese Physics Letters*, vol. 23, no. 8, pp. 2165–2168, 2006.

[13] P. G. Ganesan, K. McGuire, H. Kim et al., "ZnO nanowires by pulsed laser vaporization: synthesis and properties," *Journal of Nanoscience and Nanotechnology*, vol. 5, no. 7, pp. 1125–1129, 2005.

[14] V. V. Kireev, L. N. Dem'Yanets, L. E. Li, and V. V. Artemov, "Growth of thin ZnO films by ultrasonic spray pyrolysis," *Inorganic Materials*, vol. 46, no. 2, pp. 154–162, 2010.

[15] P.-C. Chang, Z. Fan, D. Wang et al., "ZnO nanowires synthesized by vapor trapping CVD method," *Chemistry of Materials*, vol. 16, no. 24, pp. 5133–5137, 2004.

[16] A. Dev, S. Chaudhuri, and B. N. Dev, "ZnO 1-D nanostructures: low temperature synthesis and characterizations," *Bulletin of Materials Science*, vol. 31, no. 3, pp. 551–559, 2008.

[17] S. A. Kamaruddin, M. Z. Sahdan, Kah-Yoong Chan, M. Rusop, and H. Saim, "Influence of post-annealing temperature on the material properties of zinc oxide nanorods," *Journal of Nanoscience and Nanotechnology*, vol. 10, no. 10, pp. 6419–6423, 2010.

[18] R. Ding, J. Liu, J. Jiang et al., "A general solution synthesis route to ZnO-based nanorod arrays on ceramic/silicon/quartz glass/metal substrates," *Science of Advanced Materials*, vol. 2, no. 3, pp. 396–401, 2010.

[19] C. H. Ahn, W. S. Han, B. H. Kong, and H. K. Cho, "Ga-doped ZnO nanorod arrays grown by thermal evaporation and their electrical behavior," *Nanotechnology*, vol. 20, no. 1, Article ID 015601, 2009.

[20] T. Sun and J. Qiu, "Fabrication of ZnO microtube arrays via vapor phase growth," *Materials Letters*, vol. 62, no. 10-11, pp. 1528–1531, 2008.

[21] G.-D. Yuan, W.-J. Zhang, J.-S. Jie et al., "Tunable n-type conductivity and transport properties of Ga-doped ZnO nanowire arrays," *Advanced Materials*, vol. 20, no. 1, pp. 168–173, 2008.

[22] R. Chander and A. K. Raychaudhuri, "Electrodeposition of aligned arrays of ZnO nanorods in aqueous solution," *Solid State Communications*, vol. 145, no. 1-2, pp. 81–85, 2008.

[23] X.-D. Gao, F. Peng, X.-M. Li, W.-D. Yu, and J.-J. Qiu, "Growth of highly oriented ZnO films by the two-step electrodeposition technique," *Journal of Materials Science*, vol. 42, no. 23, pp. 9638–9644, 2007.

[24] Z. Haibo, C. Jingbiao, C. Bingqiang, G. Ursula, B. Yoshio, and G. Dmitri, "Electrochemical deposition of ZnO nanowire arrays: organization, doping, and properties," *Science of Advanced Materials*, vol. 2, no. 3, pp. 336–358, 2010.

[25] X. Ren and C. Jiang, "Synthesis of ZnO nanotube arrays and heterostructures of Cu-ZnO coaxial nanotubes by electrodeposition-oxidation method," *Journal of Nanoscience and Nanotechnology*, vol. 10, no. 8, pp. 5093–5098, 2010.

[26] V. Srikant and D. R. Clarke, "On the optical band gap of zinc oxide," *Journal of Applied Physics*, vol. 83, no. 10, pp. 5447–5451, 1998.

[27] Z. K. Tang, M. Kawasaki, A. Ohtomo, H. Koinuma, and Y. Segawa, "Self-assembled ZnO nano-crystals and exciton lasing at room temperature," *Journal of Crystal Growth*, vol. 287, no. 1, pp. 169–179, 2006.

[28] D. C. Reynolds, D. C. Look, and B. Jogai, "Fine structure on the green band in ZnO," *Journal of Applied Physics*, vol. 89, no. 11 I, pp. 6189–6191, 2001.

[29] B. Lin, Z. Fu, and Y. Jia, "Green luminescent center in undoped zinc oxide films deposited on silicon substrates," *Applied Physics Letters*, vol. 79, no. 7, pp. 943–945, 2001.